Using spatiotemporal patterns of the arterial wall to assist treatment selection for carotid atherosclerosis

Aimilia Gastounioti, Marinos Prevenios, and Konstantina S. Nikita

School of Electrical and Computer Engineering, National Technical University of Athens, Greece, gaimilia@biosim.ntua.gr

Abstract. This work addressed a major clinical challenge, namely valid treatment planning for carotid atherosclerosis (CA). To this end, it introduced a novel computer-aided-diagnosis (CAD) scheme, which relies on the analysis of ultrasound videos to stratify patient risk. Based on Hidden Markov Models (HMM), it is guided by spatiotemporal patterns representing motion and strain activity in the arterial wall and it acts as a voice-recognition analogue. The designed CAD scheme was optimized and evaluated on a dataset of 96 high- and low-risk patients with CA, by investigating patterns with the strongest discrimination power and the optimal HMM parameterization. It was concluded that the optimized CAD scheme provides a CAD response with accuracy between 76% and 79%. The introduced CAD scheme may serve as a valuable tool in the routine clinical practice for CA toward personalized and valid therapeutic decision for the disease.

Keywords: carotid atherosclerosis; computer-aided diagnosis; ultrasound; motion patterns; Hidden Markov Models

1 Introduction

Carotid atherosclerosis (CA) is a chronic degenerative disease, gradually resulting in the formation of lesions (plaques) in the inner lining of the carotid artery. The fact that (a) CA is the main cause for stroke, (b) the morbidity, disability and mortality rates associated with stroke are increased, and (c) the current clinical practice for treatment selection (TR1: carotid revascularization or TR2: conservative therapy) has proved insufficient, poses the development of computer-aided-diagnosis (CAD) schemes for CA among the current major clinical needs [1].

Traditionally, vascular physicians select ultrasound (US) examination in diagnosis and follow-up for patients with CA. Moreover, the use of affordable imaging techniques, such as US, in CAD is a crucial factor. Therefore, US image analysis allows to upgrade the potential of a low-cost routine examination into a powerful tool for objective and personalized clinical assessment, i.e. risk stratification in atherosclerotic lesions. As a result, the development of CAD schemes,

which are based on US image analysis, is considered a grand challenge by the scientific community [2].

Although arterial wall dynamics constitute the direct mechanism for neurological disorders of CA, the role of motion features in CAD remains almost unexplored [2]. A few studies have investigated potential motion-based risk indices [3], while the incorporation of such indices in CAD schemes was recently attempted for the first time [4]. However, none of the related studies has investigated the role of motion patterns of the arterial wall in discriminating vulnerable atherosclerotic lesions.

This study focuses on arterial-wall spatiotemporal patterns, rather than mere motion indices, in an attempt to further elucidate the potential of arterial wall dynamics in CAD for CA toward enhancing validity in treatment planning. To this end, it designs a novel CAD scheme, which combines the analysis of US image sequences (videos) with Hidden Markov Models (HMM) and it is guided by spatiotemporal patterns representing kinematic and strain activity in the arterial wall. The designed CAD scheme is applied to US video recordings of 96 high- and low-risk patients with CA to identify the optimal parameterization for HMM and the spatiotemporal patterns with the strongest discrimination power.

2 Material & Methods

The proposed CAD scheme relies on ultrasound-video-based spatiotemporal patterns of the arterial wall to characterize a patient as high- or low-risk, and accordingly advise on the most suitable therapy (Fig. 1). In correspondence with a voice-recognition system, the arterial wall dynamics which account for stable or vulnerable atherosclerotic lesions vary among patients, in the same way as identical words can be pronounced in different ways by humans with different voices. The spatiotemporal patterns correspond to the words (sets of phonemes) and a lexicon attributes the label "high-risk" or "low-risk" patient (or equivalently "TR1" or "TR2") to each word. The design principles of the CAD scheme, as well as the optimization and evaluation procedures which were followed to investigate its potential, are hereafter presented in detail.

2.1 Design Issues

Motion analysis is performed for five regions of interest (ROIs) on a B-mode US video of a longitudinal section of the arterial wall (Fig. 1). The particular imaging modality allows the estimation of tissue motion in two dimensions, namely longitudinal, i.e. along the vessel axis, and radial, i.e. along the vessel radius. The five ROIs are the posterior (PWL) and anterior wall-lumen (AWL) interfaces, the plaque top (PTS) and bottom surfaces (PBS), and the plaque region which is contoured by PTS and PBS.

All pixels composing the five ROIs are selected as motion targets. From the target-wise radial and longitudinal motion waveforms which are produced using ABM_{KF-K2} [3], 146 spatiotemporal patterns (120 kinematic and 26 strain
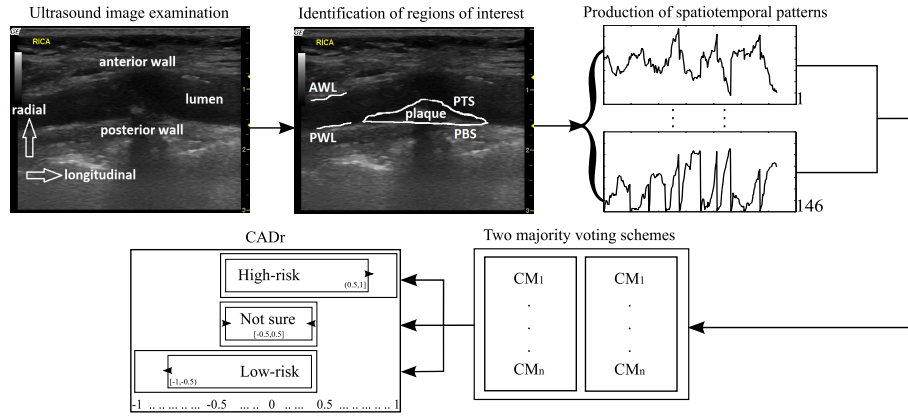
Fig. 1: Workflow for generating a CAD response (CADr) using ultrasound-video-based spatiotemporal patterns of the arterial wall. CM: classification model.

waveforms) are estimated according to the schematic representation in Fig. 2. Specifically, 24 kinematic waveforms are produced for each ROI by estimating target-wise velocity and displacement waveforms and then computing the mean and median waveforms over space (Fig. 2(a)). Based on similar steps and recently published mathematical formulas [5], strain waveforms are produced to express relative movements between (a) PWL and AWL, (b) PBS and PTS, (c) PBS and PWL or AWL, and (d) PTS and PWL or AWL (if the plaque was located at the posterior or the anterior wall, respectively), and local deformations in PWL, AWL, and PTS (Fig. 2(b)).

The stage of patient characterization as "high-risk" or "low-risk" is implemented with two majority voting schemes, each of which is fed with a subset of n spatiotemporal patterns (with $n \leq 146$) and is based on n classification models (one for each spatiotemporal pattern). Each classification model is an implementation of an HMM, a stochastic state automaton, which, if properly trained, can decode an observation sequence (word) and hence recognize its underlying patterns [6]. Due to the periodic nature of arterial wall motion, the spatiotemporal patterns are periodically reproduced. Therefore, a left-to-right HMM, consisting of five states, was considered a suitable choice [7].

The first voting scheme generates the probability of the patient belonging in the "high-risk" group (V_1), while the second one estimates the probability to be in "low-risk" (V_2). The vote of each scheme (V_j, with $j \in \{1, 2\}$) is estimated using the classification outputs, $p \in \{0 : false, 1 : true\}$, and some weights, $w \in [0, 1]$, of the classification models (eq. (1)). The final CAD response ($CADr$) is produced using eq. (2), with "-1", "0", and "1" representing "low-risk", "not sure", and "high-risk" potential results, respectively. The values of the parameters n and w were defined based on the optimization and evaluation results (for more details, see sections 2.2 and 3).
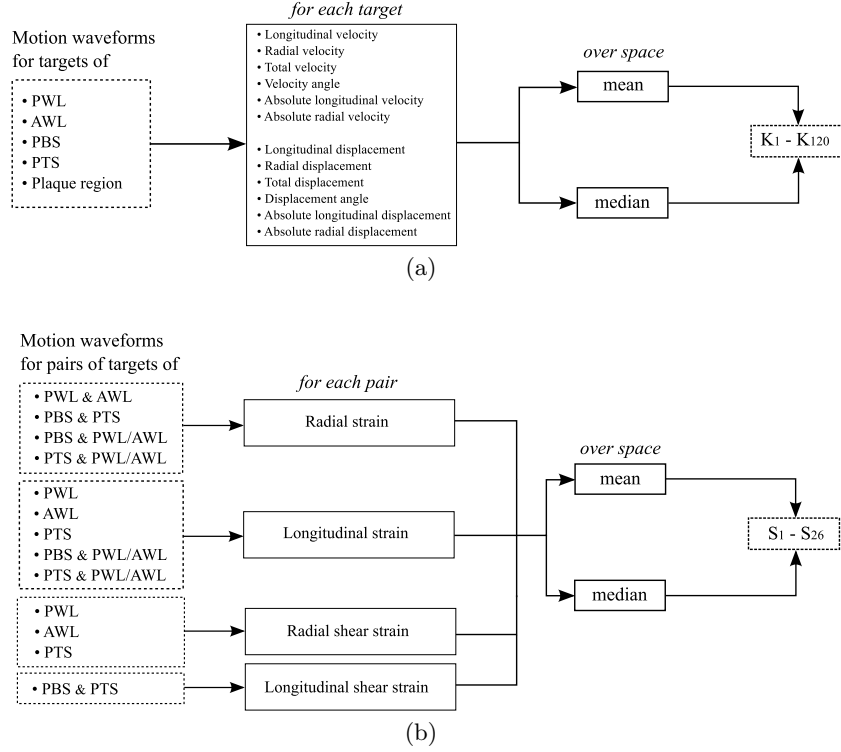
Fig. 2: Schematic representation of the production of (a) 120 kinematic and (b) 26 strain waveforms. PWL, AWL, PBS, and PTS are defined in text.

$$V_1 = \left\lceil \frac{\sum_{i=1}^{n}(p_i w_i)}{n} \right\rceil \in [0, 1], \quad V_2 = -\left\lceil \frac{\sum_{i=1}^{n}(p_i w_i)}{n} \right\rceil \in [-1, 0] \qquad (1)$$

$$CADr = round\_to\_integer\left(V_1 + V_2 \right) \in \{-1, 0, 1\} \qquad (2)$$

2.2 Optimization & Evaluation

The optimization and evaluation of the designed scheme relied on spatiotemporal patterns for 96 patients (aged $50-90$ years) with established CA (stenosis $>50\%$) [4]. For each patient, the carotid artery was scanned in the longitudinal direction according to a standardized protocol (transducer, linear array 12 MHz; dynamic range, 60 dB; persistence, low) and a B-mode US video was recorded at a rate higher than 25 frames/s for at least 3 ($2-3$ consecutive cardiac cycles). Among those patients, 20 had experienced an ischemic cerebrovascular event (stroke or transient ischemic attack) associated with the carotid stenosis ("high-risk"

group), while 76 had no neurological symptoms ("low-risk" group) within a 6-month time period from the time of examination.

HMMs were implemented using the HTK Speech Recognition Toolkit, in which input signals are first sampled and converted to Mel-frequency cepstral coefficients; training is achieved through the Baum-Welch method, which has been employed successfully in cardiovascular applications [7,8]. In this study, a separate HMM model was implemented for each type of spatiotemporal pattern and it was fed with the corresponding waveforms for all patients. Each HMM was parameterized in terms of (a) the implementation with monophones or triphones, where each word consists of three or nine phonemes, respectively, and (b) the preprocessing stage. The latter parameter involved two scenarios, in which the spatiotemporal patterns were (1) scaled and (2) not scaled in time to the maximum video duration among all patients. The optimization of each HMM lied in the maximization of the classification accuracy (i.e. percentage of correctly classified cases) for the corresponding spatiotemporal pattern, which was measured using leave-one-out cross validation [9]. In leave-one-out, a single observation (patient) is used as the testing sample, and the remaining observations compose the training dataset; this is repeated (round robin) such that each observation is used once as the testing sample.

3 Results

Fig. 3 is a graphical presentation of the maximum classification accuracy, which was achieved for each spatiotemporal pattern by the corresponding optimized HMM. The classification performance ranged between 57% and 81%, and the average performance (over the 146 spatiotemporal patterns) was 70%.
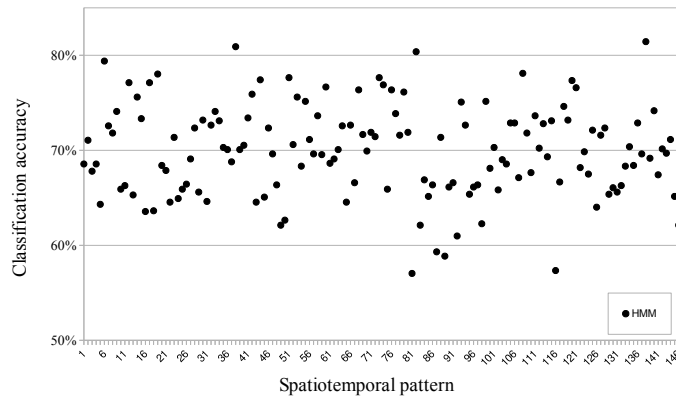

Fig. 3: Maximum classification accuracy for each type of spatiotemporal pattern of the arterial wall, using the corresponding optimized HMM.

Among all spatiotemporal patterns, we identified those with the strongest discrimination power (fig. 4), i.e. those which yielded a high ($> 75\%$) average value of specificity (i.e. correctly classified "low-risk" cases) and sensitivity (i.e. correctly classified "high-risk" cases). For those $n = 24$ spatiotemporal patterns, Table 1 includes a short description, the most suitable HMM parameterization according to the optimization procedures, and the corresponding sensitivity and specificity results.

Based on the above results, the majority voting schemes of the final CAD scheme are fed with the spatiotemporal patterns of Table 1, they consist of the corresponding optimized HMMs, and the weights w in V_1 and V_2 (eq. (1)) equal the corresponding sensitivity and specificity values, respectively.
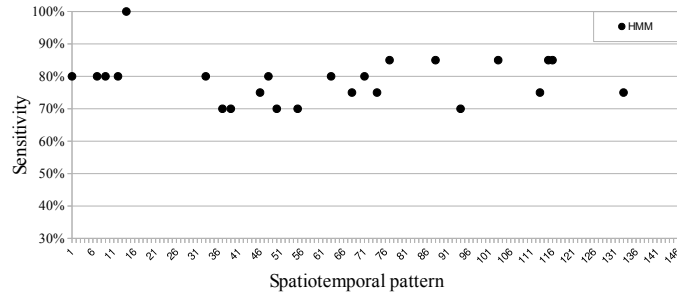
(a)
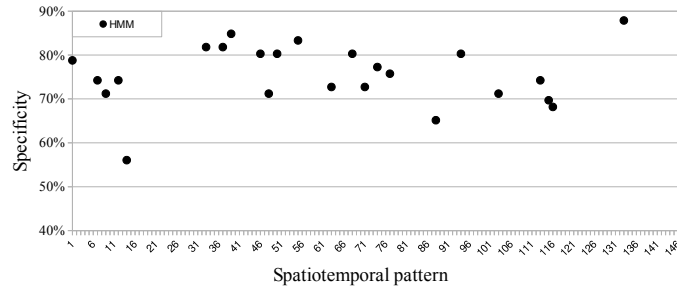
(b)

Fig. 4: Zoom in the (a) sensitivity and (b) specificity values for the spatiotemporal patterns with the strongest discrimination power.

4 Discussion

This work addressed a major clinical challenge, namely valid treatment planning for CA. In this direction, it introduced a novel image-driven CAD scheme, which

Table 1: 24 spatiotemporal patterns with the strongest discrimination power. For each case, the encoding of the pattern according to Fig. 2, a short description, and the specificity and sensitivity values which were achieved by the corresponding HMM (together with the corresponding parameterization) are presented.

Spatiotemporal pattern				Performance		HMM
#		Description		Specificity	Sensitivity	parameterization
K1	PWL	[mean]	LV	80.30%	70.00%	nt1
K18	PWL	[median] abs. RV		71.21%	85.00%	ts1
K20	PWL	[median]	RD	74.24%	75.00%	ts1
K21	PWL	[median]	TD	68.18%	85.00%	ts1
K24	PWL	[median] abs. RD		69.70%	85.00%	ts1
K36	AWL	[mean] abs. RD		87.88%	75.00%	ts1
K57	PBS	[mean]	TD	80.30%	75.00%	ts1
K60	PBS	[mean] abs. RD		83.33%	70.00%	ts1
K64	PBS	[median]	VA	72.73%	80.00%	ts1
K68	PBS	[median]	RD	72.73%	80.00%	ts1
K69	PBS	[median]	TD	77.27%	75.00%	ts1
K76	PTS	[mean]	VA	81.82%	80.00%	ts1
K88	PTS	[median]	VA	84.85%	70.00%	ts1
K90	PTS	[median] abs. RV		81.82%	70.00%	ts1
K91	PTS	[median]	LD	80.30%	75.00%	ts1
K94	PTS	[median]	TD	80.30%	70.00%	ts1
K95	PTS	[median] abs. LD		71.21%	80.00%	ts1
K100	plaque	[mean]	VA	78.79%	80.00%	nt1
K104	plaque	[mean]	RD	71.21%	80.00%	ts1
K105	plaque	[mean]	TD	74.24%	80.00%	ts1
K112	plaque	[median]	VA	74.24%	80.00%	nt1
K115	plaque	[median]	LD	56.06%	100.00%	ts1
S1	PWL & AWL	[mean]	RS	65.15%	85.00%	ts1
S18	PTS & PWL	[median]	LS	75.76%	85.00%	nt1
Average value				**76%**	**79%**	

L: longitudinal; R: radial; T: total; (for x={L,R,T}) xS: x strain; xD: x displacement; xV: x velocity; DA: displacement angle; VA: velocity angle; **HMM** {(ts1): monophones, time-scaling; (nt1): monophones, no time-scaling;};

incorporates spatiotemporal patterns of the arterial wall, in a framework of a voice-recognition analogue. This implementation allowed for elucidating the role of motion features, and in particular kinematic and strain patterns rather than mere mobility indices, in risk stratification in CA. To the best of the authors' knowledge, no similar attempts have been reported in the literature.

The proposed CAD scheme is able to assist treatment selection with accuracy between 76% and 79% (Table 1). Given the results presented by related studies in the field [2] and the CAD performance of the existing clinical practice on the same dataset [4], the aforementioned results are very encouraging for the potential of arterial-wall-motion patterns in CAD for CA. The final CAD scheme relies on 22 kinematic and 2 strain patterns which are related with the mobility of all the selected ROIs. This conclusion further reinforces the argument that the motion activity of the atherosclerotic lesion itself and healthy parts of the wall close to the lesion are equally important in risk stratification in the disease [3], [4].

A significant contribution of this study with respect to the related literature is that it suggested that the phenotype of high- and low-risk CA differs in terms of not only mobility indices describing motion properties, but also in motion trajectories and strain patterns. This conclusion remains to be further investigated in future studies on larger datasets, which will reveal the full potential of the

presented approach. In the same line of work, the effect of input variability (ex. frequency and frame rate in US image recordings) on HMM performance will be examined, as well.

In conclusion, the introduced CAD scheme may serve as a valuable tool in the routine clinical practice for CA, while it could be further enriched with other temporal features, such as the arterial pressure and heart rate. Both the design principles and the results of this study are expected to motivate the incorporation of motion analysis and spatiotemporal patterns in future related studies designing CAD tools for CA toward valid discrimination of patients in high-risk for stroke, which need to undergo carotid revascularization to prevent neurological disorders, from low-risk ones, who shoud avoid unnecessary interventions.

References

1. A. Ross Naylor, "Time to rethink management strategies in asymptomatic carotid artery disease," *Nat Rev Cardiol*, vol. 9, pp. 116–124, 2012.
2. S. Golemati, A. Gastounioti, and K. S. Nikita, "Toward novel noninvasive and low-cost markers for predicting strokes in asymptomatic carotid atherosclerosis: the role of ultrasound image analysis," *IEEE Trans Biomed Eng*, vol. 60, no. 3, pp. 652–658, 2013.
3. A. Gastounioti, S. Golemati, J. S. Stoitsis, and K. S. Nikita, "Adaptive block matching methods for carotid artery wall motion estimation from b-mode ultrasound: in silico evaluation and in vivo application," *Phys Med Biol*, vol. 58, no. 24, pp. 8647–8661, 2013.
4. A. Gastounioti, V. Kolias, S. Golemati, and et al., "Carotid - a web-based platform for optimal personalized management of atherosclerotic patients," *Comput Meth Programs Biomed*, vol. 114, no. 2, pp. 183–193, 2014.
5. S. Golemati, J. S. Stoitsis, A. Gastounioti, A. C. Dimopoulos, V. Koropouli, and K. S. Nikita, "Comparison of block-matching and differential methods for motion analysis of the carotid artery wall from ultrasound images," *IEEE Trans Inf Technol Biomed*, vol. 16, no. 5, pp. 852–858, 2012.
6. R. O. Duda, P. E. Hart, and D. H. Stork, *Pattern Classification*. Wiley Interscience, 2000.
7. R. V. Andreyo, B. Dorizzi, and J. Boudy, "Ecg signal analysis through hidden markov models," *IEEE Trans Biomed Eng*, vol. 53, no. 8, pp. 1541–1549, 2006.
8. V. Baier, M. Baumert, P. Caminal, M. Vallverdu, R. Faber, and A. Voss, "Hidden markov models based on symbolic dynamics for statistical modeling of cardiovascular control in hypertensive pregnancy disorders," *IEEE Trans Biomed Eng*, vol. 53, no. 1, pp. 140–143, 2006.
9. P. Refaeilzadeh, L. Tang, and H. Liu, *Cross-Validation. Encyclopedia of Database Systems*. Springer US, 2009.